

# Determining Stress in Translucent Materials Using Quantum Optics and Photoelasticity

Chavakorn Pruksirisombat\*, Rukdee Kaewpadung, Kitisak Boonkham  
*Mahidol Wittayanusorn School, Phutthamonthon, Nakhon Pathom, Thailand*

*\*Email: chavakorn.pru\_g33@mwit.ac.th*

## Abstract

Stress is a fundamental parameter in engineering, directly related to the strength and performance of materials. In practice, stress is often distributed unevenly within a material, although objects with identical geometries may exhibit similar stress behavior. The conventional technique for visualizing and estimating stress is photoelasticity, which relies on observing stress-induced fringes pattern. Despite its usefulness, photoelasticity is limited to regions where fringes appear and suffers from relatively low resolution. To address these limitations, this work proposes an experimental setup employing quantum optics principles to enhance stress measurement in translucent materials. The approach utilizes polymethyl methacrylate (PMMA) plates, which exhibit birefringence under applied stress. The resulting phase difference between two optical paths is used as the basis for stress determination. Entangled photon pairs and coincidence counting are incorporated to improve measurement resolution and suppress noise, thereby extending the capability beyond that of traditional photoelasticity. Experimental results demonstrate that the developed setup can detect the applied force by analyzing real-time coincidence counts. However, it does not yet provide precise quantitative stress values or detailed stress distributions. These limitations arise primarily from instrumental inaccuracies and resolution constraints, which lead to deviations from theoretical predictions. Further refinement is required for broader application.

**Keywords:** Stress, Photoelasticity, Correlated Photons Pair, Coincidence

## I. INTRODUCTION

In engineering practice, designers must account for the load-bearing capacity of materials to prevent material failure, fracture or irreversible deformation rendering the material unusable (Boston University, n.d.). Material failure can arise from various causes, one of which is stress concentration (Corrosionpedia, 2018). Stress may be classified into two main types: compressive stress, which occurs when an applied force acts inward on a material, and tensile stress, which arises when the applied force acts outward (Olson, n.d.).

Stress analysis can be conducted through three main approaches: analytical stress analysis, numerical stress analysis, and experimental stress analysis. Analytical stress analysis is grounded in the theory of elasticity, providing precise solutions using mathematical methods. However, its application is limited to specific problem types that can be solved using advanced mathematics. Numerical stress analysis, in contrast, is highly efficient as it leverages computational methods to quickly approximate solutions, though these

results are only estimates. Experimental stress analysis, while more resource-intensive, is considered the most accurate and physically interpretable, making it indispensable in practical applications. Among the widely used experimental methods is photoelasticity (Pinit, 2009).

Quantum technology has recently emerged as one of the most promising and transformative technologies, expected to have an impact comparable to the digital revolution. Quantum physics investigates phenomena at atomic and subatomic scales (on the order of nanometers), such as single photons, and has revealed properties that differ fundamentally from those of macroscopic objects (Vanita, n.d.).

Motivated by these advancements, this study explores the development of an experimental apparatus for stress analysis of transparent materials. By integrating quantum optics with the principles of photoelasticity, the objective is to improve the resolution and reliability of stress measurements beyond the limitations of conventional technique.

## II. METHODS

### 1. The Stress-Inducing Apparatus

A polymethyl methacrylate (PMMA) plate with dimensions of  $5 \times 50 \times 60 \text{ mm}^3$  was prepared for the experiment. Two circular holes with diameters of 6 mm and 8 mm were drilled at both the top and bottom ends of the plate, each hole positioned 2 mm from the edge. The PMMA specimen was mounted on an aluminum base and secured with a Dual-Range Force Sensor, as shown in Figure 1. To apply tension, a pulley was fixed to the upper arm of the aluminum frame, while a turnbuckle was attached to its lower section. A cable was looped from the Force Sensor through the pulley and connected to the turnbuckle. By tightening the turnbuckle, the tension in the cable increased, thereby inducing stress in the PMMA plate. The applied tensile load was monitored in real time by the calibrated Dual-Range Force Sensor mounted inline with the cable.

The experimental setup is illustrated in Figure 2. An industrial laser was installed on an optical table and directed through an iris diaphragm to reduce background light. The beam then passed through Polarizer 1, which was adjusted to  $45^\circ$ , producing a polarized beam at this orientation. A mirror was positioned after the polarizer to reflect the beam into a Beta Barium Borate (BBO) crystal. The BBO divided the beam into two separate paths, each deviating by  $3^\circ$ . These outputs produced correlated photon pairs at 810 nm, double the original wavelength, with the two photons being identical.



**Figure 1.** Construction of the Stress Measurement Apparatus

The two optical paths were designated as Path A and Path B. The BBO was set at  $0^\circ$  to ensure the emerging photons were polarized at  $90^\circ$ .

In Path A, the photons were redirected by a prism toward Polarizer 2, which was set at  $90^\circ$ . Afterward, Quarter-Wave Plate 1, set at  $0^\circ$ , was positioned before the stressed PMMA plate, through which the photons passed at the selected stress region. The photons then traveled through Quarter-Wave Plate 2, also set at  $0^\circ$ , and Polarizer 3, set at  $90^\circ$ , maintaining linear polarization at  $90^\circ$ . These photons were collected by Detector A, connected via an optical fiber to a Single-Photon Counting Module (SPCM) for signal detection.

In Path B, the photons first passed through Polarizer 4, which was set at  $90^\circ$ , and then entered Detector B. This detector was also connected via an optical fiber to another SPCM. Both SPCMs were linked to a coincidence circuit, which was connected to a computer for coincidence counting.

The SPCMs produce electrical pulses with a temporal width of approximately 25 ns, and the coincidence circuit was operated with a matching 25 ns coincidence window. This corresponds to a maximum tolerable optical path-length difference of approximately 7.5 m in free space. Since the actual path-length difference between Path A and Path B was orders of magnitude smaller, the resulting temporal delay did not exceed the coincidence window, and photon correlations were preserved.

The experiment began by activating the industrial laser and aligning all optical components according to the described configuration. Stress was applied incrementally to the PMMA plate using the stress-inducing apparatus, starting at 0 N and increasing to 25 N in steps of 5 N. At each force level,

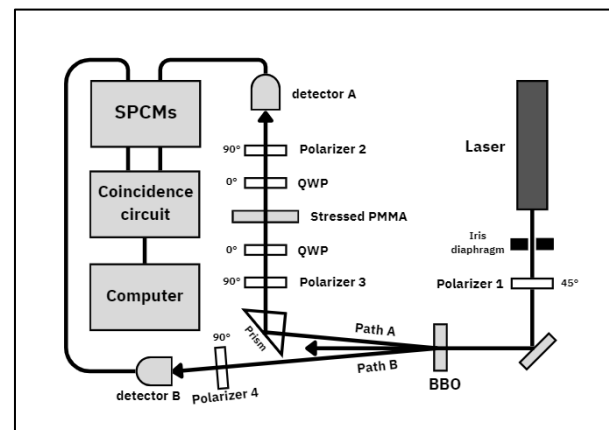


**Figure 2.** Experimental Procedure

coincidence counts were recorded over a 10-second interval, repeated three times, and the average values were calculated for subsequent analysis.

**2. Data analysis**

The experimental procedure described above yielded coincidence counts corresponding to different levels of force applied to the PMMA specimen. To ensure accuracy, three measurements were recorded for each force level, and the average coincidence counts were calculated to minimize random fluctuations. These average values served as the foundation for the subsequent analysis.

The relationship between coincidence counts and applied stress was modeled by considering the birefringence property of the PMMA plate under load. As the PMMA specimen experienced mechanical stress, the phase difference between the fast and slow axis of the transmitted light was altered. This effect was reflected in the measured coincidence counts, which could be expressed as:

$$N_l = N_p [1 - \sin^2 \frac{\delta}{2} \sin^2 2\varphi] + N_b \quad (1)$$

where  $N_l$  denotes the coincidence counts obtained from the detectors,  $N_p$  is the maximum coincidence signal,  $N_b$  is the background coincidence,  $\varphi$  is the angle that the fast axis and slow axis make with x and y axes, and  $\delta$  represents the optical phase difference induced by stress.

The stress within the PMMA plate was then calculated using the stress-optic law:

$$\delta = \frac{2\pi tc}{\lambda} (\sigma_1 - \sigma_2) \quad (2)$$

where  $(\sigma_1 - \sigma_2)$  is the stress in the specimen,  $t$  is its thickness,  $c$  is the stress-optic coefficient of PMMA, and  $\lambda$  is the wavelength of the correlated photons.

To connect the experimental results with theoretical predictions, the relationship between applied force and coincidence counts was fitted using a trigonometric model:

$$y = A[1 - \sin^2(Bx + C) \cdot \sin^2(D)] + E \quad (3)$$

where  $x$  is the applied force,  $y$  is the measured coincidence count, and  $A, B, C$  and  $D$  are fitting parameters. This model reflects the expected periodic modulation of photon coincidences caused by stress-induced birefringence.

By substituting the fitted values into Equation (2), the stress corresponding to each applied load was estimated. These calculated stress values were compared with theoretical stress distributions based on material parameters. Discrepancies between experimental and theoretical results were then examined, with particular attention to possible causes such as instrumental resolution, optical misalignment, and noise in photon counting.

**III. RESULTS AND DISCUSSION**

**1. Experimental Data**

The experimental data of coincidence counts under various applied forces are shown in Table 1 and Figure 3.

Applied Force (N)	Average Coincidence counts (counts/10s)
0	293.7
5	270.5
10	298.5
15	294.5
20	276.3
25	283.5

**Table 1.** Relationship between applied force on the PMMA plate (N) and average coincidence counts (counts/10 s).

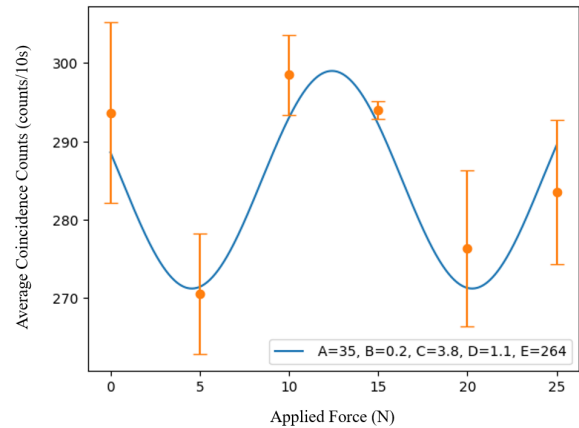


**Figure 3.** Relationship between the applied force on the PMMA plate (N) and coincidence counts within 10 seconds (counts).

The equation resulting from graph fitting is as follows:

$$y = 35[1 - \sin^2(0.2x + \sin^2(1.1))] + 264 \quad (4)$$

**2. Finding phase difference**

The phase difference was calculated by comparing the obtained equation with the equation 1. Therefore, it follows that  $0.2x + 3.8 = \frac{\delta}{2}$ . Hence,

$\delta = 0.4x + 7.6$  , where  $\delta$  represents phase difference and  $x$  is the applied force.

### 3. Finding stress value

To calculate stress value, the phase difference was substituted in the equation 2 to create a formula that explains the relationship between applied force and stress of the material:  $(\sigma_1 - \sigma_2) = 4.00 \times 10^{-5}x + 7.595 \times 10^{-4}$  where  $(\sigma_1 - \sigma_2)$  represents stress value of the material and  $x$  represents applied force.

This analytical framework demonstrates how coincidence-based quantum optical measurements can be systematically translated into stress values, establishing a foundation for future refinement of the technique.

### IV. CONCLUSION

This study successfully demonstrated the application of coincidence-based photon counting for stress analysis in transparent materials. By employing correlated photons generated from spontaneous parametric down-conversion (SPDC) and transmitting them through a stressed PMMA plate, variations in coincidence counts were observed as a function of applied force. These variations were analyzed using the stress–optic law, enabling the calculation of the principal stress difference within the specimen.

The results confirmed that the calculated stress difference increased linearly with applied force, consistent with theoretical predictions. Although minor deviations were observed between the experimental and theoretical values, these were attributed to limitations in sensor resolution, optical alignment, photon-counting noise, and material imperfections. Despite these factors, the experimental data verified the feasibility of the proposed setup.

Compared with conventional photoelasticity, which is constrained to visible fringe regions, the coincidence-counting method provides a more sensitive and versatile approach for detecting stress in transparent materials. The technique thus represents a significant step toward the integration of quantum optics with classical mechanics in material testing. Future improvements such as enhanced sensor precision, improved optical alignment, and noise suppression are expected to further refine this method.

### REFERENCES

- Andrew Olson. (n.d.). *Stress, strain, & strength: An introduction to materials science*. Science Buddies. <https://www.sciencebuddies.org/sciencefair-projects/references/stress-strain-strength-an-introduction-to-materials-science>
- Boston University. (n.d.). *Mechanics of materials: Stress*. <https://www.bu.edu/moss/mechanics-of-materials-stress>
- Corrosionpedia. (2018, July 10). *Material failure*. <https://www.corrosionpedia.com/definition/material-failure>
- Manjit, Y., Limpichaipanit, A., & Ngamjarrojana, A. (2021, August). Mechanical analysis of square-shaped PMMA using reflection photoelasticity. *Optics & Laser Technology*. <https://www.sciencedirect.com/science/article/abs/pii/S0030402621006380>
- Pinit, P. (2009). General knowledge of photoelasticity and numerical photoelasticity. *KKU Engineering Journal, 2009(363)*, 195–203. <https://www.thaiscience.info/journals/Article/TJKM/10766857.pdf>
- Sorthananusak, P. (2021, June 9). *Stress and strain*. Construction Forum. <https://constructionforum.ssi-steel.com/stress-and-strain>
- Vanita, B. (n.d.). *Quantum: The advanced technology and the answer of the future*. Digital Economy Promotion Agency (depa). <https://www.depa.or.th/th/article-view/quantum-the-new-technology>

### Acknowledgements

This paper was made possible through the guidance and support of many individuals. The authors wish to express their sincere gratitude to Dr. Kittisak Boonkham, the project advisor, for his invaluable guidance and advice throughout the development of this work, and to the project committee members Dr. Napat Kulrat, Mr. Jatuporn Pantree, and Dr. Kamonporn Kantawong for their constructive comments, questions, and suggestions that greatly improved the quality of this project. Finally, the authors would like to extend their heartfelt thanks to their parents and families for their continuous interest, encouragement, and unwavering support, which have been a constant source of strength from the beginning to the completion of this project